Conductivity of 1-Ethyl-3-Methylimidazolium Chloride (EMIC) and Aluminum Chloride ($AlCl_3$) Ionic Liquids at Different Temperatures and $AlCl_3$ Mole Fractions

ECS Transactions, 98 (10) 129-139 (2020)
10.1149/09810.0129ecst ©The Electrochemical Society

Conductivity of 1-Ethyl-3-methylimidazolium Chloride (EMIC) and Aluminum Chloride ($AlCl_3$) Ionic Liquids at different Temperatures and $AlCl_3$ Mole Fractions

Pravin S. Shinde[a], Aninda N. Ahmed[a], Md Khalid Nahian[a], Yuxiang Peng[a], and Ramana G. Reddy[a]

[a] Department of Metallurgical and Materials Engineering,
The University of Alabama, Tuscaloosa, AL 35487, USA
Corresponding author: rreddy@eng.ua.edu; Tel: 205-348-4246

The conductivity (κ) of ionic liquid (IL) comprising a melt of 1-ethyl-3-methylimidazolium chloride (EMIC) and aluminum chloride ($AlCl_3$) with different $AlCl_3$ mole fractions (X_{Al}) and temperatures (343-383 K) are reported. X_{Al} values of 0.6, 0.643, and 0.667 in EMIC-$AlCl_3$ IL are selected to maintain the desired Lewis acidity. Precise and fast conductivity measurements and the behavior of anion species in IL are studied using electrochemical impedance spectroscopy (EIS). The measured κ data followed the Arrhenius law from which the activation energies (E_a) of conduction are determined. The conductivity of EMIC-$AlCl_3$ IL decreased with the higher X_{Al}. EMIC-$AlCl_3$ with X_{Al}=0.6 exhibited higher κ (5.58 S m^{-1}) at 383 K and lowest E_a (4.25 KJ mol^{-1}) among studied compositions. Based on the thermodynamic calculations, the differences in conductivities are attributed to the interplay of anion concentration, the molecular structure, cation-anion interactions, and hydrogen bonds in the IL.

Introduction

Over the last few decades, ionic liquids (ILs) are widely investigated because of their several potential applications in catalysis, electrochemistry, synthesis, and separation processes (1-4). ILs are the solvents containing a mixture of asymmetric organic cations and organic/inorganic anions. ILs have several attractive properties such as high ionic conductivity, low vapor pressure, high thermal and electrochemical stability, and broad liquid temperature range (5-7). As a result, the ILs are continuously receiving a lot of scientific interest among the research community. However, despite a lot of progress in tuning the physical and chemical properties of ILs, the fundamental understanding of the intermolecular interaction between anions and cations is relatively unexplored (8, 9). The vital properties such as structure, diffusion, viscosity, conductivity, or melting points, depend largely on these interactions between cations and anions in ILs. We have reported several physicochemical properties such as the heat capacity (10), thermal stability (11-13), density (14, 15), viscosity (12, 14, 15), vapor pressure (15), thermal conductivity (15, 16), thermodynamic (17-19), and electroanalytical (20-23) properties of several ILs and molten salts, which are necessary to understand the electrochemistry of metals and alloys to tune their electrosynthesis parameters. In general, density, viscosity, electrochemical window, and conductivity are important physical properties that determine if an IL is suitable as an electrolyte for electrochemical devices. The conductivity (κ) is a critical

property of ILs in terms of their prospects as electrolytes for electrodeposition of metals. Electrodeposition of aluminum from imidazolium-based room-temperature chloroaluminate (RTC) ILs is one such example. Metals such as aluminum and their alloys can be electrodeposited from chloroaluminate-based electrolytes with the addition of the so1ute metal ion to the electrolyte. This can be accomplished by either anodic dissolution of the solute metal directly into the melt or addition of the appropriate chloride salt or combination of both. The RTC ILs can be obtained by combining aluminum chloride ($AlCl_3$) with certain dialkyl imidazolium chloride salts such as 1-ethyl-3-methylimidazolium chloride (EMIC). The chloro-acidity of such ILs is adjustable by controlling the mole fraction of $AlCl_3$ (X_{Al}). The ILs can be classified as acidic, neutral, and basic, depending on the $AlCl_3$ content. If $AlCl_3$ content is less (X_{Al} <0.5), the electrolyte contains $AlCl_4^-$ and Cl^- anions, exhibiting Lewis basic characteristics due to excess unbound chloride ions. On the other hand, at higher $AlCl_3$ (X_{Al} >0.5), the electrolyte possesses $AlCl_4^-$ and $Al_2Cl_7^-$ species exhibiting Lewis acidic properties mainly due to coordinately unsaturated $Al_2Cl_7^-$ species (24). Acidic RTCs are of interest as electrolytes for the electroplating of aluminum (Al) and its alloys because only the acidic compositions are active for Al plating and stripping at the anode, according to the reversible redox reaction given below (25, 26):

$$4(Al_2Cl_7)^- + 3e^- \leftrightarrow 7(AlCl_4)^- + Al \quad [1]$$

The electrochemical deposition of Al from such chloroaluminate ILs has been reported to be primarily due to contribution from the diffusion of $Al_2Cl_7^-$ species (27-29). The mobility and availability (concentration) of such anion species at the diffusion layer of respective electrodes dictate the conductivity of the electrolyte. Several researchers have studied different ILs to theoretically estimate information on ionic conductivities using rigorous methods with limited accuracy (30-38).

Fannin et al. were among the first to extensively evaluate the physical and chemical properties of dialkyl imidazolium-based ILs (39, 40). They investigated the ion-interactions as well as the phase transitions, densities, electrical conductivities, and viscosities for dialkyl imidazolium-based chloroaluminate ILs. Few other groups also investigated the electrical conductivities of such ILs. Despite several reports on the physicochemical properties, there are inconsistencies in the κ data available in the literature for imidazolium-based chloroaluminate ILs at higher temperatures (41-44). The discrepancies in conductivity values in the literature could be due to inconsistent sample purity, different measurement tools, and water contents. Thus, a systematic study on the conductivity data of imidazolium-based chloroaluminate ILs regarding electrolyte temperature and various mole fractions of $AlCl_3$ is needed. Most of the conductivity measurements in the literature have been obtained using conductivity meter probes (44-46), and the EIS technique has rarely been used for ionic liquids. The conductivity measurement by meter probes poses erroneous measurements because of several factors that include incomplete immersion of probe's surface, the boundary effects outside the electrode surfaces due to improper position of the sensor in the electrolyte, and the measurement limitation at higher temperatures. On the other hand, EIS measurement can be done in-situ in a precise manner with great accuracy even at high temperatures.

In this study, we have systematically investigated the conductivity behavior of EMIC-$AlCl_3$ ionic liquid as a function of the electrolyte composition ($AlCl_3$ mole fractions) and temperature. The conductivity of IL is studied using electrochemical impedance spectroscopy (EIS) technique to obtain accurate, non-empirical, and fast information about contributing anions on the IL conductivity. The κ values and activation energy of conduction for EMIC-$AlCl_3$ at different $AlCl_3$ mole fractions and temperatures IL determined and compared.

Experimental

Materials

The chemicals such as anhydrous $AlCl_3$ (95+%, Alfa-Aesar) and organic chloride salt 1-ethyl-3-methylimidazolium chloride (EMIC, 95%, Sigma-Aldrich) were purchased and used without further treatment. All the chemicals are heated to get rid of any moisture prior to their use for experiments. The nickel sheets (99.9%) were obtained from Sigma Aldrich company. The ultrahigh pure (UHP) Argon gas (99.999%) was obtained from Airgas.

Preparation of EMIC-$AlCl_3$ Ionic Liquid

The appropriate amount of EMIC organic chloride salt and the $AlCl_3$ were weighed for a given $AlCl_3$ mole fraction. Here, the $AlCl_3$ mole fraction of 0.667 was chosen to maximize the concentration of $Al_2Cl_7^-$ anion species in the EMIC-$AlCl_3$ IL. Both the ingredients were mixed in a Pyrex beaker on a preheated hot plate. The mixing is performed cautiously and slowly using a glass rod as the spontaneous reaction is vigorous. The mixture of two solid ingredients turns into a clear liquid as the eutectic condition is reached at room temperature. Upon stirring for 30 s, the mixture turns into a clear liquid, although few large chunks of EMIC might float in the solution, which eventually dissolves in about 30 min. The desired amount of clear IL solution is then transferred to the 50 mL electrochemical Pyrex cell placed on a hot plate, and IL was stirred for about 30 min using a magnetic stirrer at 60 RPM for homogeneous mixing at the set temperature. The IL was stored in a dry box until used for further measurements such as density and electrical conductivity. The mole fractions of $AlCl_3$, X_{Al}=0.60, 0.643, and 0.667 were chosen. Temperatures studied for EMIC-$AlCl_3$ IL at each X_{Al} were 343, 353, 363, 373, and 383 K. The UHP argon gas was purged over the surface of IL to keep it free from oxygen and moisture, and finally, the cell was sealed.

Electrical Conductivity Measurements

The electrical conductivities of EMIC-$AlCl_3$ IL at different mole fractions and temperatures were obtained using ac impedance spectroscopy through a potentiostat/galvanostat (VersaSTAT 3, M-100) in the argon environment. The conductivity experiments for ILs were performed in a two-electrode configuration with two nickel plates with identical dimensions as working and counter electrodes in a quartz cell. The working and counter electrodes are fixed in a quartz cell separated

by a distance of ~ 0.95 cm, such that one side of each electrode is tightly attached to the cell wall. Both the Ni electrodes were polished with 800 grit SiC abrasive paper, washed with ethanol and deionized water, and dried by air. The top of the cell is sealed with Teflon tape to exclude the possibility of atmospheric exposure of ionic liquid. Then, the whole-cell assembly is kept inside the oil bath on the hot-plate. The electrolyte temperature was monitored and controlled using a precision thermometer inserted into the bath. The conductivities were obtained in the temperature range of 343-383 K. The thermal equilibrium time set to measure conductivity for each given temperature was at least 30 min. The EIS curves (Nyquist plots) were obtained by applying an ac signal of amplitude 10 mV in the frequency range of 100 kHz-0.1 Hz at 0.2 V vs. Ni. The series resistance (R_s) is calculated by fitting Nyquist plots with an equivalent electrochemical circuit. Then, by using the area (A) of the electrode immersed in IL and the separation distance of electrodes (l), the conductivity (κ) is calculated using the following equation,

$$\kappa = l/R \cdot A \qquad [2]$$

Before actual conductivity measurements on ILs, the cell was calibrated by performing the EIS measurement at room temperature using three commercially available conductivity standards. The conductivity cell was carefully cleaned and dried before introducing each IL sample.

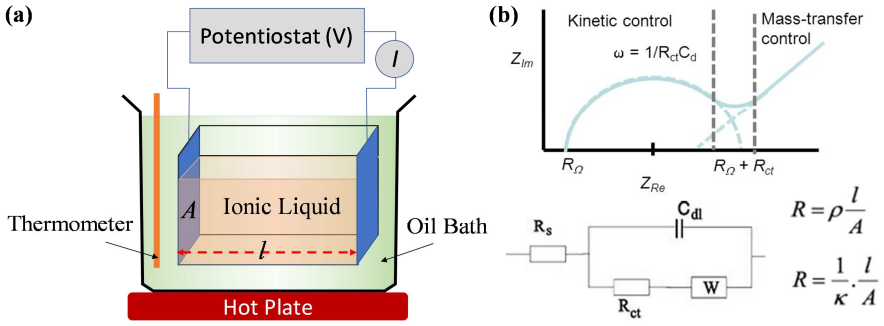

Figure 1. (a) Schematic of the experimental EIS set up. (b) Typical Nyquist plot from EIS measurement that shows a semicircle and a straight-line with an equivalent electrochemical circuit model to calculate the resistance or conductivity.

Results and Discussion

Figure 2 shows the Nyquist plots obtained for EMIC-$AlCl_3$ IL at different temperatures for the $AlCl_3$ mole fraction of 0.60. The semicircles of different diameters show up at different temperatures. The figure suggests that the diameter of arches (represented by charge transfer resistance, R_{ct}) decreases with temperature indicating faster diffusion of chloroaluminate ions in the electrolyte due to increased conductivity. Additionally, the series resistance (R_s) of the electrochemical circuit is decreasing with temperature. Before the EIS measurement of IL, the resistance of electrochemical circuits other than the electrolyte was first determined. The resistance of the cell determined using different conductivity standards as the electrolyte using the same set of Ni

electrodes and electrochemical cells was subtracted from R_s to get the actual resistance and hence to get the conductivity of the EMIC-$AlCl_3$ IL and are plotted in Figure 3.

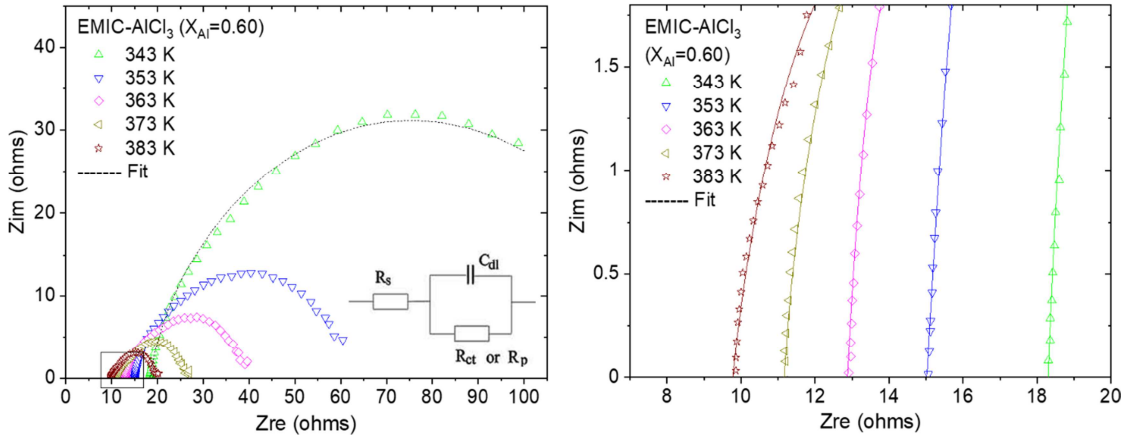

Figure 2. Nyquist plots of EMIC-$AlCl_3$ IL recorded on Ni plate vs. Ni for $AlCl_3$ mole fraction of 0.6 (left) at different temperatures and the corresponding magnified view of Nyquist plots in the high-frequency regime (right).

Figure 3 shows the temperature dependency of electrical conductivity for RTC ILs for different $AlCl_3$ mole fractions. As shown in the figure, the ionic conductivity shows an increasing trend with temperatures for all mole fractions of $AlCl_3$. Such enhancement is because of the weak attractive interaction between the ions at higher temperatures.

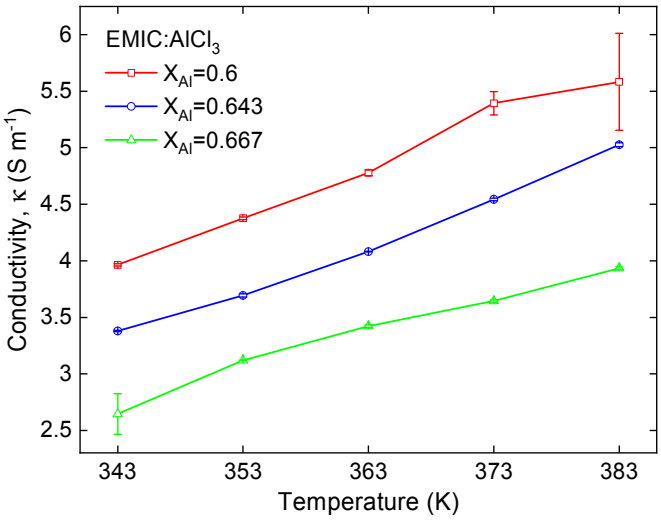

Figure 3. Conductivity plot as a function of temperature at different $AlCl_3$ mole fractions for EMIC-$AlCl_3$ IL.

All the measured conductivities are compared with literature data and are listed in TABLE I. The higher conductivity in the EMIC-$AlCl_3$ IL system has been attributed to the weaker cation-anion interaction and hydrogen bonding between $EMIC^+$-based ion pairs compared to higher alkyl-chained $HMIC^+$-based pairs (41).

TABLE I. Comparison of conductivity values obtained from EIS plots for EMIC-$AlCl_3$ IL with literature. Room temperature (RT) conductivity was obtained from the slope.

$AlCl_3$ mole fraction (X_{Al})	Conductivity, κ (S m^{-1}) at different temperatures						References
	RT	343 K	353 K	363 K	373 K	383 K	
0.6	2.43	3.96	4.38	4.78	5.39	5.58	This work
0.643	1.93	3.38	3.69	4.08	4.54	5.03	
0.667	1.61	2.65	3.12	3.42	3.64	3.94	
0.64	-	3.60	4.13	4.69	5.28	-	Fannin *et.al* (40)
0.66	-	3.40	3.91	4.44	5.00	-	
0.6	-	2.8	3.2	3.7	-	-	Ferrara *et.al* (43)
0.6	-	4.02	5.08	6.17	8.09	9.72	Vila *et.al* (44)
0.63	-	~2.5	~3.0	~3.3	-	-	

With higher mole fractions of $AlCl_3$ in EMIC-$AlCl_3$ IL, the electrical conductivities decrease in the order: $\kappa(X_{Al}=0.6) > \kappa(X_{Al}=0.643) > \kappa(X_{Al}=0.667)$. Similar behavior is found in other dialkyl imidazolium chloride chloroaluminate ILs such as MeMeImCl-$AlCl_3$, and MeBuImCl-$AlCl_3$ including EMIC-$AlCl_3$ (MeEtImCl-$AlCl_3$) (40, 41). To explain the decrease in conductivity with higher $AlCl_3$ mole fractions, it is essential to know the concentration and interplay of different anions present in the ionic liquids at a given temperature. Karpinsky et al. reported the formation of different chloroaluminate anions ($AlCl_4^-$, $Al_2Cl_7^-$, $Al_3Cl_{10}^-$, etc.) for different $AlCl_3$ mole fractions in EMIC-$AlCl_3$ (24). The equilibrium concentration (X_i) of various chloroaluminate anions in the EMIC-$AlCl_3$ IL system for different $AlCl_3$ mole fractions based on thermodynamic calculations (47) are shown in Figure 4.

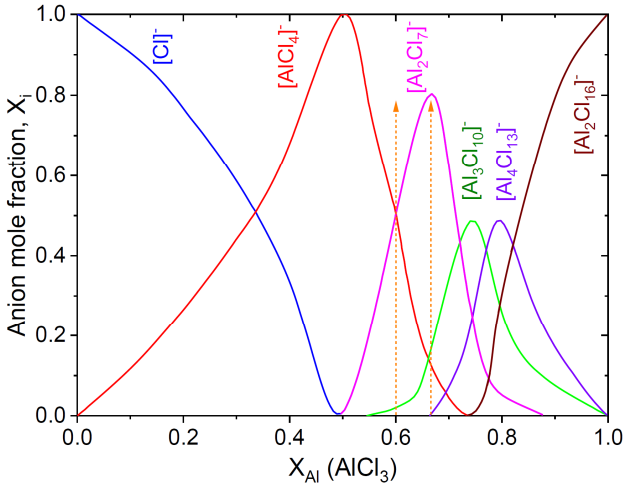

Figure 4. Equilibrium concentration (X_i) of various chloroaluminate anions (Cl^-, $AlCl_4^-$, $Al_2Cl_7^-$, $Al_3Cl_{10}^-$, $Al_4Cl_{17}^-$, and $Al_2Cl_{16}^-$) in EMIC-$AlCl_3$ IL (reproduced from (24, 47)).

As shown in Figure 4, for a studied $AlCl_3$ mole fraction range (X_{Al}=0.6-0.667), three anions, $Al_2Cl_7^-$, $AlCl_4^-$, and $Al_3Cl_{10}^-$, exist simultaneously in the IL. The relative concentrations of $Al_2Cl_7^-$ and $Al_3Cl_{10}^-$ anions increase, and that of $AlCl_4^-$ decreases with an increase in mole fraction of $AlCl_3$ from 0.6 to 0.667. At low $AlCl_3$ mole fraction (X_{Al}=0.6), an almost similar number of $Al_2Cl_7^-$ and $AlCl_4^-$ anions are present in the system. As $AlCl_3$ mole fraction increases, the concentration of $Al_2Cl_7^-$ anions increases until a maximum at X_{Al}=0.667 while the concentration of $AlCl_4^-$ anions decrease. At

higher $AlCl_3$ mole fractions, the cation-anion interaction and hydrogen bonding are reported to be stronger between $EMIC^+$ and $AlCl_4^-$ than that between $EMIC^+$ and $Al_2Cl_7^-$, due to a smaller volume and higher geometric symmetry of the $AlCl_4^-$ anion than the $Al_2Cl_7^-$ anion. Thus, the structural features make $AlCl_4^-$ more conductive in EMIC-$AlCl_3$ ionic liquid at the same conditions. This is the viable reason for the decrease in conductivity at higher mole fractions of $AlCl_3$ in EMIC-$AlCl_3$ IL. The actual concentration of these anions can be determined using mole fractions of these anions from Figure 4 and the formula weights of primary ingredients used to make the ionic liquid. The actual concentration of anions can be calculated in the following manner. The concentration of total anions ($Al_2Cl_7^-$, $AlCl_4^-$, and $Al_3Cl_{10}^-$, etc.) present in the IL are given by:

$$C_{total} = \frac{W_{total} \cdot W_{Al}}{W_{AlCl_3}}\ mol\ m^{-3} \quad [3]$$

where W_{total} is the measured weight of known volume (x mL) of EMIC-$AlCl_3$ for a given $AlCl_3$ mole fraction, W_{Al} is the weight% of $AlCl_3$ in the electrolyte, W_{AlCl_3} is the formula weight of $AlCl_3$ (133.34 g mol^{-1}). Then, the concentration of a specific anion, such as $Al_2Cl_7^-$, from the total concentration of anions (C_{total}) in EMIC-$AlCl_3$ (for a given $AlCl_3$ mole fraction, X_{Al}=0.6) electrolyte can be calculated as,

$$[Al_2Cl_7]^- = \frac{C_{total} \cdot X_{[Al_2Cl_7]^-}}{n_{[Al_2Cl_7]^-}}\ mol\ m^{-3} \quad [4]$$

where $X_{Al_2Cl_7^-}$ is the mole fraction of $Al_2Cl_7^-$ anion from equilibrium concentration data of anions (Figure 4) and $n_{Al_2Cl_7^-}$ represents the number of moles of $AlCl_3$ necessary to produce one mole of $Al_2Cl_7^-$ anion (n=2 in this case). The concentrations of $AlCl_4^-$, $Al_2Cl_7^-$ and $Al_3Cl_{10}^-$ anions determined using this method for EMIC-$AlCl_3$ for all the $AlCl_3$ mole fractions are tabulated in TABLE II.

TABLE II. Calculation of $AlCl_4^-$, $Al_2Cl_7^-$, and $Al_3Cl_{10}^-$ anion concentrations in EMIC-$AlCl_3$ IL electrolyte at different $AlCl_3$ mole fractions at 373 K. Here, n=1, 2, and 3 for $AlCl_4^-$, $Al_2Cl_7^-$, and $Al_3Cl_{10}^-$, respectively.

$AlCl_3$ mole fraction (X_{Al})	**Density of IL (g cm^{-3})**	**Total Conc. (mol m^{-3})**	**Anion mole fraction**			**Anion concentration (mol m^{-3})**		
			$AlCl_4^-$	**$Al_2Cl_7^-$**	**$Al_3Cl_{10}^-$**	**$AlCl_4^-$**	**$Al_2Cl_7^-$**	**$Al_3Cl_{10}^-$**
0.6	1.359	5.657	0.5037	0.4842	0.0121	2.850	1.370	0.023
0.643	1.387	6.176	0.2102	0.7321	0.0577	1.298	2.261	0.119
0.667	1.402	6.409	0.0918	0.7908	0.1174	0.588	2.534	0.251

The concentration of $Al_2Cl_7^-$ anions in EMIC-$AlCl_3$ IL increases while that of $AlCl_4^-$ decreases with increasing $AlCl_3$ mole fractions from 0.6 to 0.667. EMIC-$AlCl_3$ IL with 0.6 mole fraction (X_{Al}=0.6) possess maximum $AlCl_4^-$ concentration (2.839 mol m^{-3}).

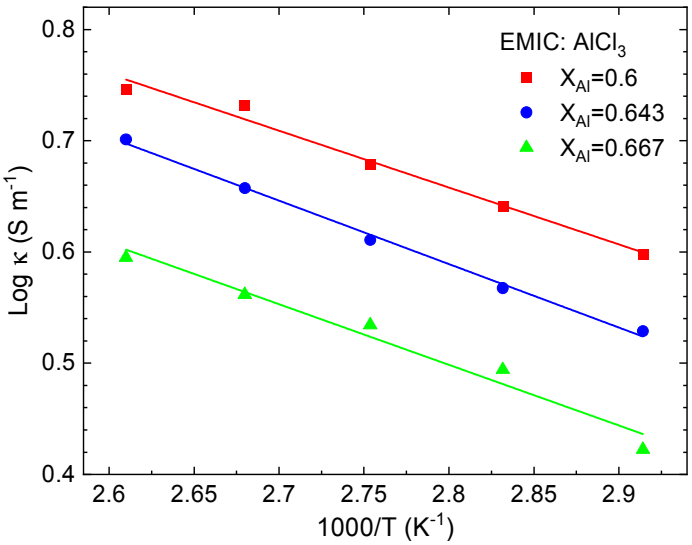

Figure 5. Arrhenius plots of EMIC-$AlCl_3$ IL with different $AlCl_3$ mole fractions.

In the literature, the effects of temperature on the electrical conductivity of ionic liquid electrolytes have been correlated by the Vogel−Tamman−Fulcher (VTF) equation (48). The experimental measurements show that the electrical conductivity follows the VTF model like literature for EMIC-$AlCl_3$ (43) as well as a typical Arrhenius law reported for several molten salts (49). Better least-square fits for the experimental data were observed with the Arrhenius plot than that of the VTF plot. The Arrhenius equation has been utilized to describe the temperature dependence of electrical conductivity as (50),

$$\kappa = A \exp\left[\frac{-E_a}{RT}\right] \qquad [5]$$

where A is the pre-exponential factor, E_a is the activation energy for ion transportation by migration, and R is the gas constant. The obtained conductivity data were fitted as a function of temperature using a linear fit of (ln κ) versus (1000/T). The experimental Arrhenius plots of the conductivities for all the ionic liquids with different $AlCl_3$ mole fractions are shown in Figure 5.

TABLE III. Activation energies obtained from Arrhenius plots for EMIC-$AlCl_3$ IL with different $AlCl_3$ mole fractions.

Ionic Liquid	$AlCl_3$ mole fraction (X_{Al})	Activation Energy (E_a), KJ mol^{-1}	References
EMIC-$AlCl_3$	0.6	4.250 ± 0.305	This work
	0.643	4.744 ± 0.172	
	0.667	4.533 ± 0.456	
	0.6	6.793	*Vila et. al.* (44)

TABLE III lists the activation energy (E_a) values determined from the slope of Arrhenius plots for EMIC-$AlCl_3$ IL with different $AlCl_3$ mole fractions. The table suggests that the activation energy of electrical conduction varies with temperature. Higher the activation energy, the slower will be the chemical reaction. EMIC-$AlCl_3$ IL gives the activation energy in the range of 4.25-10.9 kJ mol^{-1}. The E_a values increase

with $AlCl_3$ mole fraction. Thus, the findings suggest that EMIC-$AlCl_3$ ionic liquid with a 0.6-mole fraction of $AlCl_3$ can serve as an efficient electrolyte for Al-electrodeposition based on higher electrical conductivity and the lowest activation energy of conduction. The calculated activation energies are slightly less than the literature. The E_a value obtained by fitting the VTF model of conduction for EMIM-$AlCl_3$ ionic liquid with the $AlCl_3$ mole fraction of 0.60 is 6.793 kJ mol^{-1} (44).

Conclusions

In conclusion, the electrochemical impedance spectroscopy (EIS) tool was successfully used to obtain the electrical conductivities of imidazolium-based chloroaluminate ionic liquids at different temperatures (343-383 K) and different $AlCl_3$ mole fractions (0.6-0.667). The electrical conductivities of EMIC-$AlCl_3$ ionic liquid increased with temperature following an Arrhenius relationship. However, the conductivity of the EMIC-$AlCl_3$ ionic liquid is decreased at all the studied temperatures with increasing $AlCl_3$ concentration, possibly due to the depleted concentration of $AlCl_4^-$ anions, which have better structural features, such as smaller volume and higher geometric symmetry, in comparison to $Al_2Cl_7^-$ anions. The decrease in conductivity despite a larger concentration of highly conducting $Al_2Cl_7^-$ anions is attributed to the increase in internal resistance and strong cation-anion interactions in EMIC-$AlCl_3$, leading to suppressed movement of ions. A more detailed study involving the interaction of anions with high alkyl-group cations on the conductivity behavior is needed to gain further insights, which will be our future study. The experimentally obtained conductivities and activation energies of EMIC-$AlCl_3$ ionic liquid are compared with the literature data.

Acknowledgments

The authors acknowledge the financial support from the National Science Foundation (NSF) Award Number 1762522, Department of Energy (DOE) RAPID Manufacturing Institute and ACIPCO for this research project. Authors also thank the Department of Metallurgical and Materials Engineering, the University of Alabama, for providing the experimental and analytical facilities.

References

1. M. Galinski, A. Lewandowski and I. Stepniak, *Electrochim. Acta*, **51**(26), 5567 (2006).
2. J. Dupont, R. F. de Souza and P. A. Z. Suarez, *Chem. Rev.*, **102**(10), 3667 (2002).
3. X. Han and D. W. Armstrong, *Acc. Chem. Res.*, **40**(11), 1079 (2007).
4. W. S. Miao and T. H. Chan, *Org. Lett.*, **5**(26), 5003 (2003).
5. A. Marciniak and E. Karczemna, *J. Phys. Chem. B*, **114**(16), 5470 (2010).
6. C. M. Wang, H. M. Luo, H. R. Li and S. Dai, *Phys. Chem. Chem. Phys.*, **12**(26), 7246 (2010).
7. T. L. Greaves and C. J. Drummond, *Chem. Rev.*, **108**(1), 206 (2008).

8. D. R. MacFarlane, M. Forsyth, E. I. Izgorodina, A. P. Abbott, G. Annat and K. Fraser, *Phys. Chem. Chem. Phys.*, **11**(25), 4962 (2009).
9. H. Weingaertner, *Angew. Chem. Int. Ed.*, **47**(4), 654 (2008).
10. J. D. Holbrey, W. M. Reichert, R. G. Reddy and R. D. Rogers, in *Ionic Liquids as Green Solvents: Progress and Prospects,* , R. D. Rogers and K. R. Seddon Editors, p. 121, ACS Symposium Series 856, American Chemical Society, New York (2003).
11. V. Kamavaram and R. G. Reddy, *Int. J. Therm. Sci.*, **47**(6), 773 (2008).
12. V. Kamavaram and R. G. Reddy, in *Light metals 2005*, H. Kvande Editor, p. 501, Warrendale (2005).
13. Ramana G. Reddy, Zhijing Zhang, Mario F. Arenas and Daniel M. Blake, *High. Temp. Mater. Proc.*, **22**(2), 87 (2003).
14. V. Karmavaram and R. G. Reddy, in *Aluminum 2003*, S. K. Das Editor, p. 299 (2003).
15. Y. Peng and R. G. Reddy, in *Advances in Molten Slags, Fluxes, and Salts: Proceedings of the 10th International Conference on Molten Slags, Fluxes and Salts 2016*, p. 1169 (2016).
16. T. Wang, S. Viswanathan, D. Mantha and R. G. Reddy, *Sol. Energy Mater. Sol. Cells*, **102**, 201 (2012).
17. R. Reddy, A. Yahya and L. Brewer, *J. Alloys Compd.*, **321**(2), 223 (2001).
18. M. Zhang, V. Kamavaram and R. G. Reddy, *J. Phase Equilib. Diff.*, **26**(2), 124 (2005).
19. M. M. Zhang and R. G. Reddy, *Min. Proc. Ext. Met.*, **119**(2), 71 (2010).
20. A. Liu, Z. Shi and R. G. Reddy, *Ionics*, **26**(6), 3161 (2020).
21. A. Liu, Z. Shi and R. G. Reddy, *Electrochim. Acta*, **251**, 176 (2017).
22. A. Liu, Z. Shi and R. G. Reddy, *J. Electrochem. Soc.*, **164**(9), D666 (2017).
23. M. Li, Z. Wang and R. G. Reddy, *J. Electrochem. Soc.*, **161**(4), D150 (2014).
24. Z. J. Karpinski and R. A. Osteryoung, *Inorg. Chem.*, **23**(10), 1491 (1984).
25. T. Jiang, M. J. Chollier Brym, G. Dubé, A. Lasia and G. M. Brisard, *Surf. Coat. Technol.*, **201**(1), 1 (2006).
26. J. S. Wilkes, J. A. Levisky, R. A. Wilson and C. L. Hussey, *Inorg. Chem.*, **21**(3), 1263 (1982).
27. D. Pradhan and R. G. Reddy, *Mater. Chem. Phys.*, **143**(2), 564 (2014).
28. T. Jiang, M. C. Brym, G. Dubé, A. Lasia and G. Brisard, *Surf. Coat. Technol.*, **201**(1-2), 1 (2006).
29. J. Tang and K. Azumi, *Electrochim. Acta*, **56**(3), 1130 (2011).
30. A. P. Abbott, *ChemPhysChem*, **6**(12), 2502 (2005).
31. S. Tsuzuki, H. Tokuda, K. Hayamizu and M. Watanabe, *J. Phys. Chem. B*, **109**(34), 16474 (2005).
32. H. Matsuda, H. Yamamoto, K. Kurihara and K. Tochigi, *J. Comput. Aided Chem.*, **8**, 114 (2007).
33. J. M. Slattery, C. Daguenet, P. J. Dyson, T. J. S. Schubert and I. Krossing, *Angew. Chem. Int. Ed.*, **46**(28), 5384 (2007).
34. K. Tochigi and H. Yamamoto, *J. Phys. Chem. C*, **111**(43), 15989 (2007).
35. O. Borodin, *J. Phys. Chem. B*, **113**(36), 12353 (2009).
36. K. Ueno, H. Tokuda and M. Watanabe, *Phys. Chem. Chem. Phys.*, **12**(45), 15133 (2010).

37. P. Eiden, S. Bulut, T. Kochner, C. Friedrich, T. Schubert and I. Krossing, *J. Phys. Chem. B*, **115**(2), 300 (2011).
38. S. Tsuzuki, *ChemPhysChem*, **13**(7), 1664 (2012).
39. A. A. Fannin, L. A. King, J. A. Levisky and J. S. Wilkes, *J. Phys. Chem.*, **88**(12), 2609 (1984).
40. A. A. Fannin, D. A. Floreani, L. A. King, J. S. Landers, B. J. Piersma, D. J. Stech, R. L. Vaughn, J. S. Wilkes and J. L. Williams, *J. Phys. Chem.*, **88**(12), 2614 (1984).
41. Y. Zheng, K. Dong, Q. Wang, J. Zhang and X. Lu, *J. Chem. Eng. Data*, **58**(1), 32 (2013).
42. J. Lu and D. Dresinger, in *Ionic Liquids as Green Solvents Progress and Prospects*, R. D. Rogers and K. R. Seddom Editors, p. 495, American Chemical Society, Washington, DC (2003).
43. C. Ferrara, V. Dall'Asta, V. Berbenni, E. Quartarone and P. Mustarelli, *J. Phys. Chem. C*, **121**(48), 26607 (2017).
44. J. Vila, P. Gines, J. M. Pico, C. Franjo, E. Jimenez, L. M. Varela and O. Cabeza, *Fluid Phase Equilibria*, **242**(2), 141 (2006).
45. H. Xu, T. Bai, H. Chen, F. Guo, J. Xi, T. Huang, S. Cai, X. Chu, J. Ling, W. Gao, Z. Xu and C. Gao, *Energy Storage Mater.*, **17**, 38 (2019).
46. G. Zhu, M. Angell, C.-J. Pan, M.-C. Lin, H. Chen, C.-J. Huang, J. Lin, A. J. Achazi, P. Kaghazchi, B.-J. Hwang and H. Dai, *RSC Adv.*, **9**(20), 11322 (2019).
47. H. Øye, M. Jagtoyen, T. Oksefjell and J. Wilkes, in *Materials Science Forum*, p. 183 (1991).
48. B. S. Lalia, N. Yoshimoto, M. Egashira and M. Morita, *J. Power Sources*, **195**(21), 7426 (2010).
49. J. O. M. Bockris and A. K. N. Reddy, Modern Electrochemistry 2, in, Plenum Press, New York (1970).
50. H. Every, A. Bishop, M. Forsyth and D. R. Macfarlane, *Electrochim. Acta*, **45**(8-9), 1279 (2000).